High-resolution angle-resolved photoemission spectroscopy of CeBi

H. Kumigashira, S.-H. Yang, T. Yokoya, A. Chainani, T. Takahashi, A. Uesawa, T. Suzuki, and O. Sakai
Department of Physics, Tohoku University, Sendai 980-77, Japan

Y. Kaneta
Department of Quantum Engineering and Systems Science, Faculty of Engineering, The University of Tokyo, Tokyo 113, Japan
(Received 4 March 1996)

High-resolution angle-resolved photoemission spectroscopy (HR-ARPES) has been performed on a CeBi single crystal to study the complicated electronic structure near the Fermi level (E_F). The experimental result was compared with the band-structure calculation based on the p-f mixing model as well as the de Haas–van Alphen (dHvA) effect measurements. It was found that the overall feature of the valence band shows a remarkably good agreement between the experiment and the calculation, suggesting the essential validity of the p-f mixing model. HR-ARPES measurement near E_F has established the existence of a small electron pocket centered at the M point in the Brillouin zone, supporting the band calculation and the dHvA measurement. HR-ARPES spectra around the Γ point show some dispersive bands near E_F indicative of a hole pocket centered at the Γ point, though it was not so clearly resolved as the electron pocket due to close proximity of individual bands. These results are consistent with the semimetallic nature of CeBi. The observed quantitative discrepancy between the experiment and the calculation is discussed. [S0163-1829(96)00437-7]

I. INTRODUCTION

Cerium monopnictides (CeX; X=N, P, As, Sb, and Bi) with a simple NaCl structure are categorized as a low-carrier dense-Kondo system, showing anomalous physical properties such as complicated magnetic phase transitions.[1–7] Many experimental and theoretical studies have been performed on these compounds to elucidate the nature of their anomalous electronic and magnetic properties. Among several theoretical proposals, the p-f mixing model[8] seems successful in explaining well the unique magnetic behavior. According to this model, the top of occupied electronic states consists mainly of the pnictogen np state (n=2–6), while the bottom of the unoccupied electronic states originates in the Ce $5dt_{2g}$ state. Ce monopnictides except for CeN are semimetallic due to the overlap between the pnictogen p state and the Ce $5dt_{2g}$ state, possessing a hole pocket with a dominant pnictogen p character at the Γ point (Γ_8) and an electron pocket with the Ce $5d$ nature at the X point in the Brillouin zone. It is established that Ce ions in Ce monopnictides are almost trivalent and the Ce $4f_{5/2}$ state is split into the Γ_8 quartet and the Γ_7 doublet due to the crystal field. Hence the pnictogen p states forming the top of occupied electronic states are strongly mixed with the Ce $4f_{5/2}$ quartet having the same Γ_8 symmetry, causing a downward shift of the Ce $4f_{5/2}(\Gamma_8)$ state and at the same time an upward shift of the pnictogen $p_{3/2}$ state. On the other hand, the intra-atomic anisotropic d-f Coulomb interaction is expected to be considerably strong between the Ce $4f_{5/2}$ doublet (Γ_7) and the Ce $5dt_{2g}$ band at the bottom of the unoccupied state. The p-f mixing model thus explains how the complicated electronic structure near the Fermi level (E_F) gives an anomalously high Kondo temperature[4,9] (T_K) as well as the anomalous anisotropic magnetic properties.

CeBi is expected to have the largest hole and electron pockets among Ce monopnictides[8] because of the strongest spin-orbit interaction of Bi $6p$ states and the weakest hybridization between Bi $6p$ and Ce $4f$ states.[10–13] Experimentally, it behaves as a low-carrier (0.021 carriers per a Ce ion) dense-Kondo system.[14,15] It shows a complicated magnetic phase transition with temperature; it transform from a paramagnetic phase to an antiferromagnetic type-I phase (AF-I) at 25 K, then changes into another antiferromagnetic-type-IA phase (AF-IA) at 13 K.[1,2] The Ce $4f$ spin arrangement in the antiferromagnetic phases is described by the periodic stacking structure of ferromagnetic planes with alternating up (+) and down (−) magnetization. The above-mentioned AF-I and AF-IA phases of CeBi correspond to stacking sequences of (+−) and (++−−) of ferromagnetic planes, respectively. The paramagnetic phase shows a dense-Kondo-like behavior with the Kondo temperature of T_K=100 K,[3,4] in spite of the low-carrier concentration. The de Haas–van Alphen (dHvA) measurement on the ferromagnetic phase[9,16] shows an overall agreement with the band-structure calculation based on the p-f mixing model.[9,17–19]

Angle-resolved photoemission spectroscopy (ARPES) is a unique and powerful experimental technique, providing directly the E (energy) $-\mathbf{k}$ (wave vector) relation, namely the band structure of a crystal. In this paper, we report our high-resolution ARPES results on single-crystal CeBi at low temperature (10 K). We compare the ARPES results with the band-structure calculation as well as the dHvA measurements and discuss the complicated electronic structure of CeBi.

II. EXPERIMENTAL

CeBi single crystals were grown by the Bridgman method with a sealed tungsten crucible and a high-frequency induction furnace. High purity Ce ($3N$) and Bi ($5N$) metals with the respective composition ratio were used as starting materials. The obtained sample were characterized by the Debye-

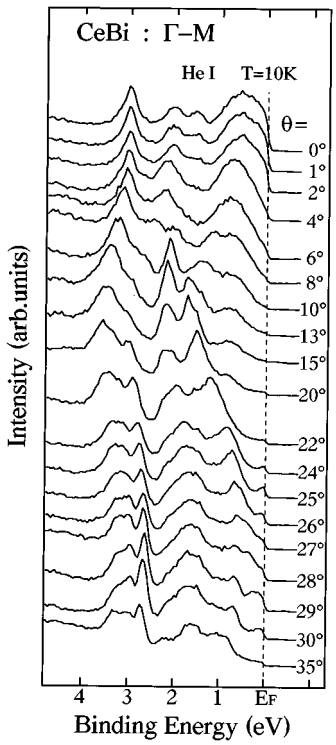

FIG. 1. High-resolution angle-resolved photoemission spectra of a CeBi single crystal measured in the Γ-*M* direction with the He I resonance line (21.22 eV) at 10 K. Polar angle (θ) referred to the surface normal is indicated on each spectrum.

Scherrer method as well as the resistivity and transversal magnetic resistance measurements. Obtained lattice constant, residual resistivity at 4.2 K, and magnetoresistivity $[\Delta\rho/\rho(0)$ where $\Delta\rho=\rho(10\mathrm{T})-\rho(0)]$ at 0.8 K were 6.505 Å, 1.0 $\mu\Omega$ cm, and 8. These values are almost the same as those of a single crystal with which the dHvA effect was observed,[9,16,20] showing a high quality of the present crystal.

Photoemission measurements were carried out using a homebuilt high-resolution photoemission spectrometer, which has a large hemispherical electron energy analyzer (diameter: 300 mm) and a highly bright discharge lamp.[21] The base pressure of the spectrometer was 2×10^{-11} Torr and the angular resolution was about $\pm1°$. The energy resolution was set at about 50 meV for quick data acquisition because of relatively fast degradation of the sample surface as described below. A clean mirrorlike surface of CeBi [100] plane was obtained by *in situ* cleaving at 10 K just before the measurement and kept at the same temperature throughout the measurement. Since we observed degradation of the sample surface as evident by increase of background in the spectrum, we recorded every spectra before the spectral change became detectable (within a few hours). We have measured ARPES spectra for several samples and obtained reproducible results. The Fermi level of the sample was referred to that of a gold film evaporated on the sample substrate and its accuracy was estimated to be better than 5 meV.

III. RESULTS AND DISCUSSION

Figure 1 shows the ARPES spectra of CeBi measured at $T=10$ K along the Γ*M* direction in the Brillouin zone (see Fig. 2 for the Brillouin zone). The spectral intensity is normalized at a prominent peak around 3 eV binding energy. The polar angle (θ) denoted on each spectrum was measured from the surface normal of the [100] plane. We find in Fig. 1 that the position and intensity of peaks in the ARPES spectra are very sensitive to the polar angle. This spectral change directly represents the band structure of CeBi in the Γ*M* direction, since the polar angle θ is converted into the wave vector **k**. When we look at the vicinity of the Fermi level, we notice that the spectral change is remarkable at $\theta=0°-10°$ and 22°–35°. In the region of $\theta=0°-10°$, a large broad peak moves from the vicinity of the Fermi level to the high binding-energy side when we increase the polar angle from 0° to about 10°. On the other hand, we find a small but distinct structure just at E_F in spectra of $\theta=22°-35°$. The former spectral change suggests the existence of dispersive bands which touch or cross E_F near the Γ point in the Brillouin zone while the latter implies an electron pocket near the *M* point.

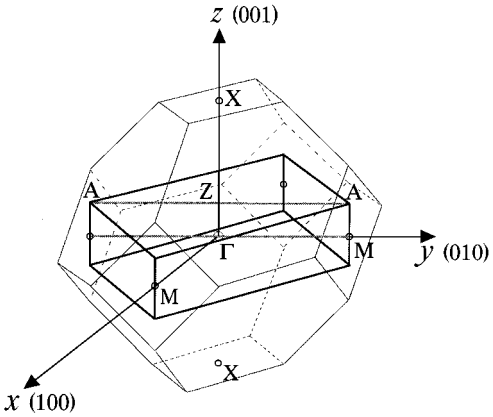

FIG. 2. Brillouin zone of an antiferromagnetic CeBi of type-IA (AF-IA) phase with a simple tetragonal structure (thick line) compared with that of the paramagnetic phase with a fcc structure (thin line).

In order to see the spectral change near E_F in detail, we show in Fig. 3 the spectra near E_F in an enlarged binding-energy scale. We find in Fig. 3(a) that there are at least two dispersive bands (*A* and *B*) in the vicinity of the Fermi level around $\theta=0°$ and both have a similar energy dispersion with the minimum binding energy at $\theta=0°$. The observed dispersion appears to be symmetric with respect to $\theta=0°$, which indicates high accuracy of the sample alignment in the present measurement. We also find in Fig. 3(a) that band *A* does not cross E_F, while band *B* seems to touch E_F near $\theta=0°$ since the photoemission spectrum shows a very sharp rise at E_F at $\theta=-1°-2°$. In the region of larger polar angles [Fig. 3(b)], on the other hand, we observed three well-resolved bands (*X*-*Z*), of which dispersive features are totally different each other in contrast with the region near $\theta=0°$ [Fig. 3(a)]. In particular, band *Z* shows a very characteristic energy dispersion; it suddenly appears at E_F at $\theta=24°-25°$, showing a very small dispersion with the maximum binding energy of about 0.15 eV at $\theta=29°$ and again enters into unoccupied states (above E_F) at $\theta=35°$. This provides a clear evidence for existence of an electron pocket at

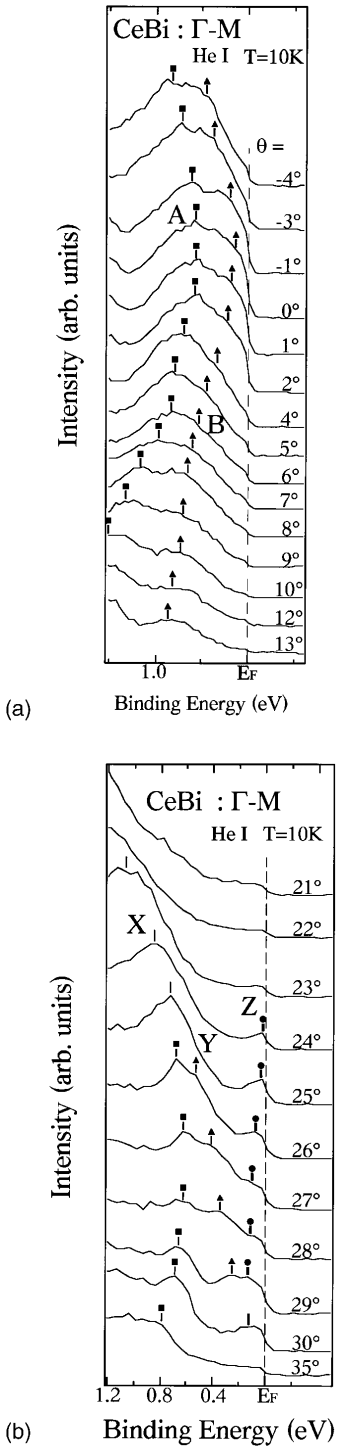

FIG. 3. (a) High-resolution angle-resolved photoemission spectra near E_F of CeBi in an enlarged binding-energy scale measured around the $\Gamma(Z)$ point in the Brillouin zone. Spectra show dispersive bands $A(\blacksquare)$ and $B(\blacktriangle)$. Band B approaches E_F and touches it around $\theta=0°$. (b) High-resolution angle-resolved photoemission spectra near E_F of CeBi around the $M(A)$ point in the Brillouin zone. Three dispersing bands $X(\blacksquare)$, $Y(\blacktriangle)$, and $Z(\bullet)$ are clearly seen. Note that band Z suddenly appears at E_F around $\theta=24°-25°$, showing a slight energy dispersion with the maximum binding energy of about 0.15 eV at $\theta=29°$ [corresponding to the $M(A)$ point], and then enters again into unoccupied states at $\theta=35°$. This characteristic behavior of band Z indicates existence of an electron pocket at the M point.

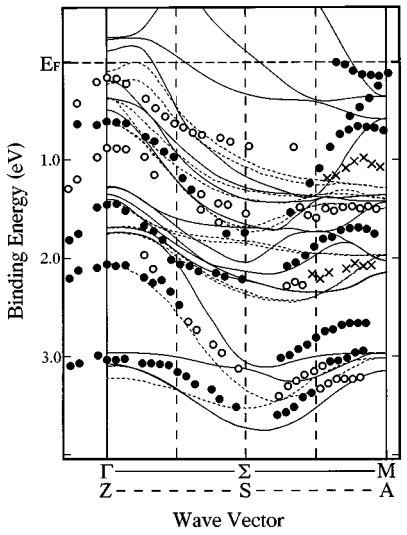

FIG. 4. Experimental band structure of CeBi in the ΓMAZ plane of the Brillouin zone (Fig. 2) derived from the present ARPES measurements (Figs. 1 and 3). Solid and open circles and crosses represent prominent, medium, and weak structures in the spectra, respectively. The result of the band-structure calculation based on the p-f mixing model is also shown for comparison. Solid and broken lines correspond to ΓM and ZA lines in the Brillouin zone, respectively. Note an overall agreement between the experiment and the calculation.

the M point in the Brillouin zone as predicted by the band-structure calculation.[18,22]

Figure 4 shows the band dispersion obtained from the present ARPES measurement by converting the polar angle into the wave vector **k** using a conventional method.[23] The experimental results are shown by solid and open circles and crosses depending on the intensity of peaks in the spectra; solid circles represent prominent peaks, being followed by open circles and crosses in this order. In Fig. 4, the experimentally obtained band dispersion is compared with a band-structure calculation based on the p-f mixing model. In the calculation, we assumed that the up-spin and down-spin sites are occupied by the $j_z=5/2$ and $j_z=-5/2$ states of a Ce ion, respectively. The energy level of the occupied state was set at 1.2 eV below the E_F in the calculation as in the ferromagnetic case. The details of the band calculation was described elsewhere.[18] In Fig. 4, we show the calculated energy dispersion along two parallel high-symmetry lines ΓM (solid lines) and ZA (broken lines) since the ARPES measurement was done in the ΓMAZ plane in the Brillouin zone (see Fig. 2). It is well established that a high-symmetry line in the Brillouin zone has a dominant contribution to the ARPES spectrum in a three-dimensional material because of the relatively high density of states on it and the lifetime broadening of **k** perpendicular to the crystal surface.[23]

As found in Fig. 4, the overall feature of the band structure shows a good agreement between the experiment and the calculation. It is surprising that the binding energy of bands at $\Gamma(Z)$ point shows an almost perfect agreement between the two. We also find that some highly dispersive bands located at 2–3.5 eV predicted by the calculation are clearly observed in the present ARPES measurement at almost the same energy position, although a small deviation is

seen near the $M(A)$ point. A bunch of calculated bands located at 1.5–2 eV is also observed in the experiment as a prominent peak. According to the band calculation,[8,9,16,18,19] the dispersive bands located at 1.5–3.5 eV originate mainly in the Bi $6p_{1/2}$ state. Although we could not resolve each calculated band located at $E_F-1.5$ eV because of their close proximity and the lifetime broadening, we observed one or two composite band(s) in the experiment in the same energy region. These bands have a dominant Bi $6p_{3/2}$ character.[8,9,16,18,19] In Fig. 4, we find a small portion of a dispersive band below E_F at the M or A point, which we ascribe to an electron pocket at the M point predicted by the band calculation since there are no corresponding calculated bands near E_F at the A point. It is noticed that the E_F-crossing point of this electron pocket shows a good agreement between the calculation and the ARPES experiment, supporting the dHvA measurement,[9,16] while the bottom of the electron pocket is shallower about twice in the experiment, suggesting a strong renormalization effect near E_F. This electron pocket consists of the Ce $5dt_{2g}$ states.[8,9,16,18,19]

When we compare the present ARPES result with the dHvA measurement,[9,16,20] bands A and B in Figs. 3(a) and 4 may correspond to the bands forming the small hole sheets observed in the dHvA measurement for the ferromagnetic phase under a magnetic field. The p-f mixing model has predicted that the anisotropic p-f (Γ_8) mixing pushes up the β bands, producing several hole pockets centered at Γ point under a magnetic field. In the present ARPES study, however, we could not observe the larger hole sheets.[20] This may be because the spectral intensity is considerably suppressed by a strong anisotropic p-f (Γ_8) mixing and the resultant small photoionization cross section for the He I photons.[24]

While it is difficult to identify definitely a hole pocket at the Γ point, an electron pocket at the M point is clearly observed in the experiment as seen in Fig. 4. However, we could not observe another larger electron pocket which crosses E_F around a middle point between the Γ and M points. According to the p-f mixing model,[8,9,19] this band has a strongly mixed character of Ce $4f$ and $5d$ states with a substantial $4f$ weight. Similarly to the large hole pocket which has a strong $4f$ character and is absent in the present ARPES measurement, the large electron pocket may not appear as a prominent structure in an ARPES spectrum due to its considerably small photoionization cross section for He I photons.[24]

Finally, we discuss the quantitative discrepancy between the experiment and the calculation as shown in Fig. 4. Although both show a good qualitative agreement each other, we find some discrepancies in the binding energy of bands, for example, at the $M(A)$ point. This quantitative difference may arise from the treatment of the f band in the calculation, where a single level is assumed for the f level and an appropriate binding energy was chosen to reproduce the dHvA result. However, as already observed by resonant photoemission spectroscopy,[10,12] the f level in the compound splits into the bonding and antibonding bands with the energy interval of 2–3 eV. This suggests that the observed discrepancy in Fig. 4 may be reduced when two separate f levels are properly incorporated in the calculation.

IV. CONCLUSION

We have performed a high-resolution angle-resolved photoemission spectroscopy (ARPES) on a single crystal CeBi to investigate the complex electronic structure near E_F. We found that ARPES spectra show a remarkable change with respect to the angle of emitted photoelectrons, reflecting the complicated band structure. Although we found some dispersive bands with a Bi $6p_{3/2}$ character which approach and touch E_F at the Γ point indicative of existence of a hole pocket centered at the Γ point, we could not resolve each band due to the close proximity of individual bands. In contrast, we clearly observed an electron pocket at the M point having a strong Ce $5dt_{2g}$ character. These ARPES observations confirm the semimetallic nature of CeBi. We also found that the band-structure calculation based on the p-f mixing model shows a good qualitative agreement with the present ARPES result, indicating the essential validity of the model. The observed quantitative discrepancy between the experiment and the calculation demands a more realistic treatment of the $4f$ level in the calculation.

ACKNOWLEDGMENTS

We are very grateful to Professor T. Kasuya for useful discussion. T.Y. and A.C. thank the Japan Society for the Promotion of Science for financial support. This work was supported by grants from the NEDO and the Ministry of Education, Science, and Culture of Japan.

[1] H. Bartholin, P. Burlet, O. Quezal, J. Rossat-Mignod, and O. Vogt, J. Phys. (Paris) **40**, 130 (1979).

[2] T. Kasuya, Y. S. Kwon, T. Suzuki, K. Nakanishi, F. Ishiyama, and K. Takegahara, J. Magn. Magn. Mater. **90&91**, 389 (1990).

[3] M. Sera, T. Suzuki, and T. Kasuya, J. Magn. Magn. Mater. **31–34**, 385 (1983).

[4] H. Kitazawa, I. Oguro, M. Hirai, Y. Kondo, T. Suzuki, and T. Kasuya, J. Magn. Magn. Mater. **47&48**, 532 (1985).

[5] J. M. Leger, K. Oki, D. Ravot, J. Rossat-Mignod, and O. Vogt, J. Magn. Magn. Mater. **47&48**, 277 (1985).

[6] N. Môri, Y. Okayama, H. Takahashi, Y. S. Kwon, and T. Suzuki, J. Appl. Phys. **69**, 4696 (1991).

[7] N. Môri, Y. Okayama, H. Takahashi, Y. Haga, and T. Suzuki, Physica B **186–188**, 444 (1993).

[8] For example, T. Kasuya, Y. Haga, Y. S. Kwon, and T. Suzuki, Physica B **186–188**, 9 (1993); T. Kasuya, A. Oyamada, M. Sera, Y. Haga, and T. Suzuki, *ibid.* **199&200**, 585 (1994), and references therein.

[9] T. Kasuya, O. Sakai, J. Tanaka, H. Kitazawa, and T. Suzuki, J. Magn. Magn. Mater. **63&64**, 9 (1987).

[10] A. Franciosi, J. H. Weaver, N. Mårtensson, and M. Croft, Phys. Rev. B **24**, 3651 (1981).

[11] J. W. Allen, S.-J. Oh, I. Lindau, J. M. Lawrence, L. I. Johanson, and S. B. Hagström, Phys. Rev. Lett. **46**, 1100 (1981).

[12] S.-J. Oh, S. Suga, Y. Saito, A. Kakizaki, T. Ishii, M. Taniguchi, A. Fujimori, T. Miyahara, H. Kata, A. Ochiai, T. Suzuki, and T.

Kasuya, Solid State Commun. **82**, 581 (1992).
[13] M. Takeshige, O. Sakai, and T. Kasuya, J. Magn. Magn Mater. **52**, 363 (1985).
[14] T. Kasuya, Y. Haga, T. Suzuki, Y. Kaneta, and O. Sakai, J. Phys. Soc. Jpn. **61**, 3447 (1992).
[15] T. Suzuki, Physica B **186–188**, 347 (1993).
[16] H. Kitazawa, T. Suzuki, M. Sera, I. Oguro, A. Yanase, A. Hasegawa, and T. Kasuya, J. Magn. Magn. Mater. **31–34**, 421 (1983).
[17] A. Hasegawa, J. Phys. Soc. Jpn. **54**, 677 (1985).
[18] O. Sakai, Y. Kaneta, and T. Kasuya, Jpn. J. Appl. Phys. **26**, 477 (1987).
[19] O. Sakai, M. Takeshige, H. Harima, K. Otaki, and T. Kasuya, J. Magn. Magn. Mater. **52**, 18 (1985).
[20] K. Morita (private communication).
[21] T. Yokoya, T. Takahashi, T. Mochiku, and K. Kadowaki, Phys. Rev. B **51**, 3945 (1995).
[22] Y. Kaneta *et al.* (unpublished).
[23] F. J. Himpsel, Adv. Phys. **32**, 1 (1983).
[24] J. J. Yeh and I. Lindau, At. Data Nucl. Data Tables **32**, 1 (1985).